Electronic Supplementary Material (ESI) for Chemical Communications
This journal is © The Royal Society of Chemistry 2012

Electronic Supplementary Information

for

Design, Synthesis and Evaluation of Small Molecule Reactive Oxygen Species Generators as Selective *Mycobacterium tuberculosis* Inhibitors

Allimuthu T. Dharmaraja,[a] Mallika Alvala,[b] Dharmarajan Sriram,[b] Perumal Yogeeswari[b] and Harinath Chakrapani[a,]*

[a]Indian Institute of Science Education and Research Pune, Pune 411 008, India. Fax: (+) 91-20-2589-9790 [b]Department of Pharmacy, Birla Institute of Technology & Science-Pilani, Hyderabad Campus, Jawahar Nagar, Hyderabad 500 078, India

*E-mail: harinath@iiserpune.ac.in.

This journal is © The Royal Society of Chemistry 2012

Synthesis and Characterization

General. All reactions were conducted under a nitrogen atmosphere. All chemicals were purchased from commercial sources and used as received unless stated otherwise. Dichloromethane (DCM), toluene and tetrahydrofuran (THF) for reaction were used as dried, and petroleum ether and ethyl acetate (EtOAc) for chromatography were distilled before use. Column chromatography was performed on Merck silica gel (100–200 mesh). ^{1}H and ^{13}C spectra were recorded on JEOL 400 MHz (or 100 MHz for ^{13}C) spectrometers using either residual solvent signals as an internal reference ($CDCl_3$ δ_H, 7.24 ppm, δ_C 77.1 ppm) or an internal tetramethylsilane (δ_H = 0.00, δ_C = 0.0). Chemical shifts (δ) are reported in ppm and coupling constants (*J*) in Hz. The following abbreviations are used: m (multiplet), s (singlet), br s (broad singlet), d (doublet), t (triplet) dd (doublet of doublet) and dt (doublet of triplet). High-resolution mass spectra were obtained from HRMS-ESI-Q-Time of Flight LC/MS or MALDI TOF/TOF analyzer (Applied Biosystems 4800 Plus). FT-IR spectra were obtained using NICOLET 6700 FT-IR spectrophotometer as KBr disc and reported in cm^{-1}. Melting point was measured using a VEEGO melting point apparatus; all melting points were measured in open glass capillary and values are uncorrected. High performance liquid chromatography (HPLC) was performed on a Dionex ICS-3000 model or a Metrohm 882 compact IC plus instrument equipped with a Phenomenex C-18 reverse phase column (250 × 4.6 mm, 5µm). Fluorimetric, luminometric and spectrophotometric measurements were performed using Thermo Scientific Varioscan microwell plate reader. All theoretical calculations, geometry optimization and vibrational analyses were performed at the DFT B3LYP/6-31G(d,p) level for all these structures using Gaussian 03 software. The purity of all compounds synthesized in this study was ≥ 95% as determined by HPLC and/or elemental analysis. Compounds **1**,[1] **2**,[2-3] **3**,[4-5] **4**,[2-3] **5**,[6-7] **9**,[8] **10**,[9-10] **11**,[11-13] and **12**[9] have been previously reported and analytical data that we collected were consistent with the reported values.

General procedure for [4 + 2] cycloaddition with 1, 3-cyclopentadiene. To a solution of 1,4-naphthoquinone (1.0 mmol) in dichloromethane (10 mL), freshly distilled 1,3-cyclopentadiene (1.2 mmol) was added and the reaction mixture was stirred at room temperature. The reaction progress was

monitored by thin layer chromatography (TLC). After completion of the reaction the volatiles were evaporated under reduced pressure to obtain crude product, which was purified by silica gel column chromatography using solvent system of ethyl acetate (1→ 5%) and pet ether to afford pure material.

General procedure for [4 + 2] cycloaddition with 1, 3-cyclohaxadiene. To a solution of the 1,4-naphthoquinone (1.44 mmol) in toluene (10 mL), freshly distilled 1,3-cyclohexadiene (1.72 mmol) was added and the mixture was refluxed for 12 h. Upon complete consumption of the starting material (TLC analysis), the reaction mixture was evaporated to dryness under reduced pressure to obtain crude product. The crude material was purified by silica gel column chromatography using ethyl acetate (1→5 %) and petroleum ether solvent system to obtain pure material.

5,8-Dihydroxy-1,4,4a,9a-tetrahydro-1,4-ethano-9,10-anthraquinone (6). Starting from 5,10-dihydroxy-1,4-naphthoquinone (100 mg, 0.53 mmol), compound **6** was isolated as a bright yellow crystalline solid (101 mg, 71%): mp 133 – 135 °C; FT-IR (ν_{max}, cm^{-1}): 3428, 1621, 1449; ^{1}H NMR (400 MHz, $CDCl_3$): δ 12.59 (s, 2H), 7.19 (s, 2H), 6.19 (dd, *J* = 3.2, 6.1 Hz, 2H), 3.36 (d, *J* = 1.4 Hz, 2H), 3.15 (s, 2H), 1.77 (dd, *J* = 5.5, 13.2 Hz, 2H), 1.40 (dd, *J* = 4.2, 11.8 Hz, 2H); ^{13}C NMR (100 MHz, $CDCl_3$): δ 203.6, 155.9, 133.8, 128.4, 114.7, 49.7, 36.2, 24.9; Elemental analysis for $C_{16}H_{14}O_4$ calcd. C, 71.10; H, 5.22. Found C, 71.28; H, 5.03; HRMS (MALDI) for $[C_{16}H_{14}O_4+K]^+$: calcd., 309.0529. Found: 309.0168.

5-benzyloxy-1,4,4a,9a-tetrahydro-1,4-methano-9,10-anthraquinone (7). Starting from 5-benzyloxy-1,4-naphthoquinone (50 mg, 0.19 mmol), compound **7** was isolated as a pale yellow semi-solid (36 mg, 58%): FT-IR (ν_{max}, cm^{-1}): 1641, 1574, 1451, 1378, 1281; ^{1}H NMR (400 MHz, $CDCl_3$): δ 7.49-7.54 (m, 4H), 7.37-7.40 (m, 2H), 7.28-7.32 (m, 1H), 7.20-7.22 (m, 1H), 6.06 (dd, *J* = 2.8, 5.6 Hz, 1H), 5.99 (dd, *J* = 2.8, 5.6 Hz, 1H), 5.20 (dd, *J* = 12.3, 20.9 Hz, 2H), 3.58 (d, *J* = 13.1 Hz, 2H), 3.46 (dq, *J* = 3.5, 12.5 Hz, 2H), 1.55 (dt, *J* = 1.7, 8.7 Hz, 1H), 1.47 (d, *J* = 8.6 Hz, 1H); ^{13}C NMR (100 MHz, $CDCl_3$): δ 198.5, 196.6, 157.8, 138.8, 136.5, 136.3, 135.8, 134.4, 128.8, 128.0, 126.9, 126.2, 119.2, 119.0, 71.0, 51.6, 50.5, 48.7, 48.1, 47.8; HRMS (ESI) for $[C_{22}H_{18}O_3+Na^+]$: calcd., 353.1154. Found: 353.1157.

5-Benzyloxy-1,4,4a,9a-tetrahydro-1,4-ethano-9,10-anthraquinone (8). Starting from 5-benzyloxy-1,4-naphthoquinone (200 mg, 0.76 mmol), compound **8** was isolated as a yellowish white semi-solid (189

mg, 72%): FT-IR (ν_{max}, cm^{-1}): 1680, 1651, 1584, 1497; ^1H NMR (400 MHz, $CDCl_3$): δ 7.49-7.53 (m, 4H), 7.36-7.40 (m, 2H), 7.28-7.32 (m, 1H), 7.19 (m, 1H), 6.09-6.19 (m, 2H), 5.20 (d, *J* = 8.0 Hz, 2H), 3.29-3.34 (m, 2H), 3.21 (s, 2H), 1.70 (d, *J* = 7.6 Hz, 2H), 1.38 (d, *J* = 8.8 Hz, 2H); ^{13}C NMR (100 MHz, $CDCl_3$): δ 198.2, 196.2, 157.3, 138.7, 136.3, 134.3, 134.2, 133.5, 128.8, 128.0, 126.9, 126.3, 119.0, 118.8, 71.0, 52.1, 51.1, 34.4, 33.6, 24.8, 24.7; HRMS (ESI) for [$C_{23}H_{20}O_3$+Na^+]: calcd., 367.1310. Found: 367.1311.

5-Hydroxy-1,2,3,4,4a,9a-hexahydro-1,4-ethano-9,10-anthraquinone (13). To a 25 mL round bottom flask containing tetrahydrofuran (THF, 6 mL), **4** (100 mg, 0.39 mmol) was added followed by Pd/C (21 mg (10 wt.%), 5 mol%); the reaction mixture was flushed with hydrogen gas using a balloon and stirred under hydrogen atmosphere at room temperature for 2 h. Upon complete consumption of starting material (TLC analysis), the reaction mixture was filtered through a celite bed and washed with THF of 10 mL. The resulting filtrate was evaporated under reduced pressure and washed with *n*-pentane (3 × 3 mL) to obtain a yellow crystalline solid (82 mg, 81%): mp 90 – 92 °C; FT-IR (ν_{max}, cm^{-1}): 3428, 2937, 1674, 1631, 1574; ^1H NMR (400 MHz, $CDCl_3$): δ 12.74 (s, 1H), 7.61-7.68 (m, 2H), 7.26 (dd, *J* = 1.7, 7.8 Hz, 1H), 3.17 (dd, *J* = 2.8, 10.7 Hz, 1H), 3.07 (dd, *J* = 3.0, 10.7 Hz, 1H), 2.36 (d, *J* = 13.7 Hz, 2H), 1.70-1.76 (m, 4H), 1.38-1.42 (m, 4H); ^{13}C NMR (100 MHz, $CDCl_3$): δ 206.3, 198.4, 162.0, 137.4, 135.2, 123.8, 118.2, 48.6, 48.1, 30.3, 30.0, 25.9, 25.8, 22.0, 21.9; Elemental analysis for $C_{16}H_{16}O_4$ calcd.: C, 74.98; H, 6.29. Found C, 75.29; H, 6.12; HRMS (MALDI) for [$C_{16}H_{16}O_3$+Na^+]: calcd., 279.0997. Found: 279.0840.

5-Hydroxy-2,3,4a,9a-tetrahydro-1,4-ethano-9,10-anthraquinone (14). To a 25 mL round bottom flask compound **13** (100 mg, 0.39 mmol) was dissolved in chloroform ($CHCl_3$, 5 mL) and DBU (50 µL, 0.33 mmol) was added drop wise to above solution. The reaction flask was stirred at room temperature for 20 min, complete conversion of the starting material was followed by thin layer chromatography (TLC). The reaction mixture was evaporated under reduced pressure to obtain crude product. The crude product was passed through a silica plug (5 cm) to obtain an orange yellow crystalline solid (29 mg, 48%): mp 141 – 143 °C; FT-IR (ν_{max}, cm^{-1}): 3479, 1631, 1575, 1454; ^1H NMR (400 MHz, $CDCl_3$): δ 12.19 (s, 1H), 7.6 (dd, *J* = 1.2, 7.5 Hz, 1H), 7.56 (t, *J* = 8.0 Hz, 1H), 7.21 (dd, *J* = 1.2, 8.3 Hz, 1H), 3.52 (s, 2H), 1.78 (d, *J* =

7.5 Hz, 4H), 1.34 (d, J = 7.6 Hz, 4H); ^{13}C NMR (100 MHz, $CDCl_3$): δ 187.1, 181.1, 161.5, 151.9, 150.4, 135.9, 132.6, 124.1, 119.1, 115.2, 27.1, 26.3, 25.3, 25.2.; HRMS (ESI) for [$C_{16}H_{14}O_3$+Na^+]: calcd., 255.1021. Found: 255.1020.

Reactive Oxygen Species Generation Studies

Luminol assay for superoxide estimation.[14-15] A luminol stock solution (4 mM) was prepared by dissolving 7.1 mg of luminol in 10 mL of 30 μM sodium hydroxide solution. To a 96-microwell plate, compound (5 μM) in quintuplicate was incubated with 180 μL of potassium phosphate buffer (100 mM, pH 7.4) and 5 μL of luminol stock solution (4 mM, in 30 μM sodium hydroxide) for 30 min at RT and luminescence was measured using microwell plate reader (Table S1).

Table S1. Measurement of superoxide generated during incubation of compounds **1**-**14** (5 μM)

Compd No	RLI (AU)	S. D.
1	187	164
2	358	102
3	217	70
4	1398	153
5	50	57
6	220	59
7	77	44
8	21	18
9	115	46
10	23	13
11	283	47
12	29	10
13	1613	265
14	91	72

RLI: Relative luminescence intensity

As a positive control superoxide ($O_2^{\bullet-}$) was generated from the enzymatic reaction of xanthine oxidase (0.1 U/mL) and hypoxanthine (1 mM in phosphate buffer pH 7.8) in the presence of 5 units catalase as a scavenger for H_2O_2; for compound **13** superoxide estimation was done in the presence of H_2O_2 scavenger (catalase, 5 units) as well. Superoxide dismutase (SOD from Bovine erythrocytes, sigma), 10 U/mL was prepared in 1 mM phosphate buffer (1 mM in phosphate buffer pH 7.8. The complete quenching of luminescence was observed during the addition of SOD.

This journal is © The Royal Society of Chemistry 2012

Estimation of hydrogen peroxide.[16-17] Xylenol orange (1.25 mM) stock solution was prepared by dissolving 9.5 mg (12.5 μmol) in 10 mL of de-ionised water. This solution was diluted 10-fold using de-ionised water to get 125 μM stock solution. A 1 M solution of sorbitol (1.82 g, 1 mol in 10 mL dI water) was also prepared and diluted to produce 100 mM stock solution. A 250 mM ferrous ammonium sulphate (FAS) solution was prepared by dissolving 980.3 mg of FAS in 10 mL of 2.5 M sulphuric acid. This solution was further diluted 10-fold by using 2.5 M sulphuric acid for the final stock solution of FAS (25 mM). Xylenol orange and sorbitol stock solutions were mixed together in a ratio of 1:1 (v/v) and to this 100:1 (v/v) FAS stock solution was added to obtain the final FOX stock solution, which is used for the hydrogen peroxide estimation. A calibration curve (See Supporting Information, Table S2) was generated with hydrogen peroxide (See Supporting Information, Figure S1). Hydrogen peroxide estimation experiments were performed in 96-microwell plates. Compound (5 μM) in triplicate was incubated at pH 7.4 with potassium phosphate buffer (20 μL, 0.5% acetonitrile for solubility) for 30 min. FOX reagent (180 μL) was added to the above, incubated for 30 min at room temperature (25° C) for the color development and the absorbance (586 nm) was measured using a Thermo Scientific Varioscan microwell plate reader.

Table S2. Calibration of H_2O_2 using FOX assay:

[H_2O_2] in μM	Abs	S. D.
0	0.0000	0.0014
1	0.0974	0.0035
2	0.2151	0.0046
3	0.3568	0.0053
4	0.4785	0.0055
5	0.5468	0.0059
6	0.6300	0.0014

Catalase from Bovine liver (1.03 mg) was dissolved in 1.0 mL of de-ionized water to obtain 2000 U/mL stock solution. 10 mL of catalase stock solution was added to 30 min reaction mixture of compound 13 (5 mM) in phosphate buffer (pH 7.4); After 5 min, FOX reagent (180 μL) was added and reacted for 30 min at RT, measured the absorbance at 586 nm. We found no significant color formation in the presence of catalase confirming the production of H_2O_2.

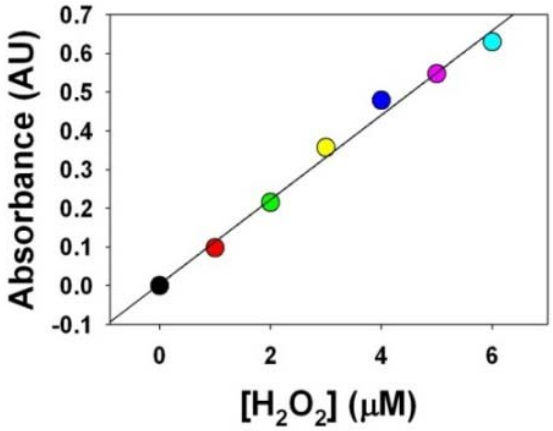

Figure S1. Calibration curve for H_2O_2 of 0 - 6 μM using FOX reagent

Table S3. Measurement of H_2O_2 generated during incubation of **1-14** (5 μM) in pH 7.4 buffer:

Compd No	Abs at 586nm (AU)	S. D.	[H_2O_2] (in μM)	% of H_2O_2
1	0.0396	0.0016	0.2572	5.1
2	0.0395	0.0028	0.2568	5.1
3	0.0671	0.0052	0.4356	8.7
4	0.0859	0.0073	0.5580	11.1
5	0.0311	0.0026	0.2021	4.0
6	0.0853	0.0081	0.5539	11.1
7	0.0362	0.0018	0.2348	4.7
8	0.0459	0.0031	0.2980	6.0
9	0.0319	0.0008	0.2074	4.1
10	0.0303	0.0047	0.1965	1.9
11	0.0798	0.0029	0.5179	10.4
12	0.0777	0.0046	0.5046	5.0
13	0.2184	0.0031	1.4182	28.4
14	0.0301	0.0066	0.1948	3.9

Table S4. Kinetics of H_2O_2 generation from Compound **13**:

Time (h)	Abs at 586nm (AU)	S. D.	[H_2O_2] (in μM)	% of H_2O_2
1	0.2849	0.0039	1.8500	37
2	0.38654	0.0037	2.5100	50.2
3	0.48818	0.0047	3.1700	63.4
4	0.5082	0.0136	3.3000	66
6	0.54516	0.0042	3.5400	70.8
8	0.54362	0.0038	3.5300	70.6
10	0.55594	0.0034	3.6100	72.2
12	0.517594	0.008	3.3610	67.22

Supercoiled plasmid DNA cleavage. DNA cleavage was analyzed by the conversion of pBR322 circular DNA to open circular and/or linear forms. Briefly, pBR322 DNA (100 ng) was incubated with compound in the presence of 1 eq. of $FeCl_2$ in 1 mM phosphate buffer (pH 8.0), in a final volume of 20 μL, the solutions were incubated at 37 °C for 6 h. The solutions were mixed with bromophenol blue (0.25 wt.%) and 1X GelRed™ (2 μL), this mixture was loaded in a 1.0% agarose gel (0.5 g in 50 mL of 1x TAE (40 mM Tris-acetate buffer containing 1 mM EDTA, pH 8.0), and immediately subjected to electrophoresis in a horizontal slab gel apparatus containing 1x TAE buffer as medium for 40 min under constant 95 V. After electrophoresis, the DNA was visualized under GBOX Syngene UV-transilluminator, photographed using Genesnap-7.04. Image analysis for quantifying the amount of DNA damage was done using Syngene-gene tools software, where the pixels of bands were quantified and analyzed.

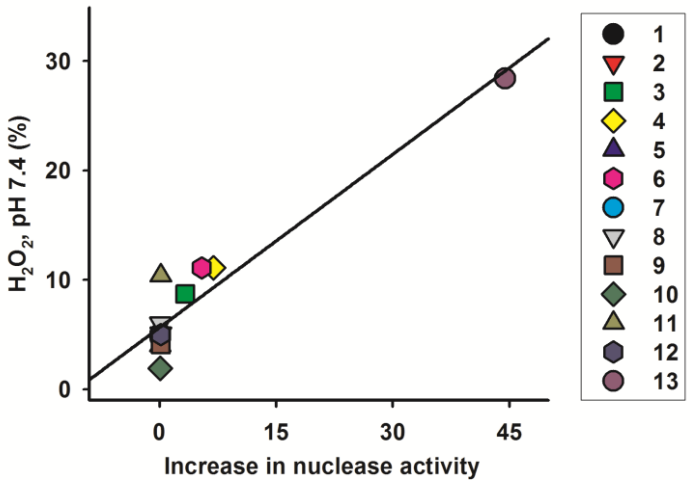

Figure S2. Comparison of DNA damage induced in the presence of Fe(II) during 6 h and hydrogen peroxide yields during 30 min. Linear regression analysis afforded a Pearson's correlation coefficient R = 0.9475, P-value < 0.0001 suggesting an excellent correlation between these variables. These results indicate the involvement of ROS in induction of DNA damage to plasmid DNA.

Extracellular H_2O_2 generation in *Mycobacterium smegmatis*.[18] The 10-acetyl-3,7-dihydroxyphenoxazine (Amplex red) solution was used to estimate hydrogen peroxide. The Amplex red solution was prepared by following the manufacturer's protocol from invtirogen-Amplex red hydrogen peroxide assay kit (100 μM Amplex red reagent and 0.2 U/mL HRP (Horse Radish Peroxidase enzyme) in 50 mM PBS (phosphate buffered saline). Using hydrogen peroxide a calibration curve was generated (See Supporting Information, Table S5, Figure S3). The cultured *Mycobacterium smegmatis* MC^2155 was centrifuged to aspirate out the media and re-suspended in LB medium of 5 mL. The bacterial medium was incubated with a final concentration of 50 μM compound in DMSO (0.5%) was placed in each well and incubated for 60 min, bacterial solution with 0.5% DMSO was used as the control. To the 96-microwell plate 50 μL of Amplex red solution was added and incubated at room temperature for 30 min. Fluorescence of resulting Amplex red dye reaction (resorufin) was measured by exciting in the range 554–566 nm and the emission was collected in the range 586–594 nm (Table S6).

Table S5. Calibration of H_2O_2 using Amplex red assay:

$[H_2O_2]$	RFI (Original)	RFI (Corrected)	S. D.
0.0	14.13677	0	0
1.0	132.4167	118.3	0.9
2.0	255.4793	241.3	6.6
4.0	481.939	467.8	5.9
6.0	687.032	672.9	5.15
8.0	868.0407	853.9	5.9
10.0	1029.007	1014.9	4.6

RFI: Relative fluorescence intensity

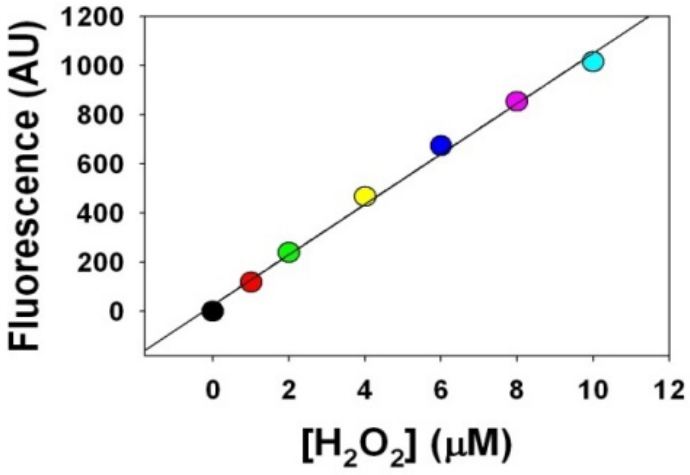

Figure S3. Calibration curve for H_2O_2 of 0-10 μM with Amplex red reagent

Table S6. Extracellular H_2O_2 measurement using Amplex red assay:

Compd No	RFI (AU)	S. D.	[H_2O_2] (in μM)	% of H_2O_2
1	192.6857	4.8833	1.8	3.6
2	224.6333	12.6070	2.1	4.2
3	309.3747	11.3385	2.9	5.8
4	363.6707	20.1115	3.4	6.8
5	103.3071	0.0424	0.96	1.9
6	228.1180	0.7616	2.16	4.3
7	133.1740	0.4808	1.24	2.5
8	223.6100	0.8026	2.09	4.2
9	139.3300	2.0117	1.30	2.6
10	107.4160	0.2814	1.00	1.0
11	136.8053	1.5104	1.28	2.6
12	235.7474	4.6280	2.20	2.2
13	587.5370	31.0031	5.50	11.0
14	206.0110	2.2422	1.92	3.8
DMSO	170.733	0.41	1.63	-

RFI: Relative fluorescence intensity

Intracellular ROS generation in *Mycobacterium smegmatis*:

Mycobacterium smegmatis MC^2155 were inoculated in a ten milliliter 60 hours cultures, grown from single colonies in Dubos medium monitored by measuring OD_{600} 0.1 - 0.5. The cultured bacteria was centrifuged to aspirate out the media and re-suspended in Lysogeny broth (LB) medium of 5 mL. The bacterial medium was incubated with 200 μM of 2′,7′-dichlorodihydrofluorescein diacetate ($DCFH_2$-DA) a pre-nonfluorescent dye for 60 min followed with centrifugation to aspirate out the $DCFH_2$-DA loading LB medium. The collected bacterial pellet was re-suspended with LB medium and 100 μL aliquots were placed in triplicate in wells of sterile flat bottom 96-well microtiter plates. A final concentration of 50 μM compound **13** in DMSO (0.5%) was added in each well and incubated for 60 min; bacterial solution with 0.5% DMSO was used as the control. The fluorescence of oxidized green fluorescent 2′,7′-dichlorofluorescein (DCF) was measured by exciting around 484 – 496 nm and the emission was collected around 524 – 536 nm wavelength (Table S7).

This journal is © The Royal Society of Chemistry 2012

Table S7. Detection of intracellular ROS generation by compounds using H_2-DCFDA:

Compound	Time (min)	RFI (AU)[(a)]	S. D.
13	30	247	15.2
	60	509.04	12.1
14	30	177.7	8.0
	60	274.0	8.4

(a) Relative fluorescence intensity (RFI) given here is subtracted from the value obtained from DMSO control treated cells.

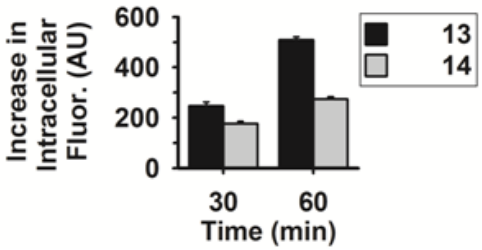

Figure S4. Increase in intracellular oxidative species upon treatment of *Msm* with **13** or **14** as determined by a 2,7-dichlorodihydrofluorescein-diacetate (DCFH-DA)-based fluorescence assay, DMSO (0.5%) was used as control. Increase in intracellular fluorescence is with respect to DMSO control.

This journal is © The Royal Society of Chemistry 2012

Stability studies of compound 13. To a 5 mL glass vial compound **13** (500 µL, 10 mM) was reacted with potassium phosphate buffer (450 µL, 100 mM) under an air balloon at 37 °C. Each time 500 µL of the reaction mixture was diluted to 5 mL using CH_3CN: H_2O (1:1 v/v) and injected into high performance liquid chromatography at different time intervals during 14 h. An authentic sample of **14** was injected as a control.

Stability studies of compound 13 under pH 7.4.

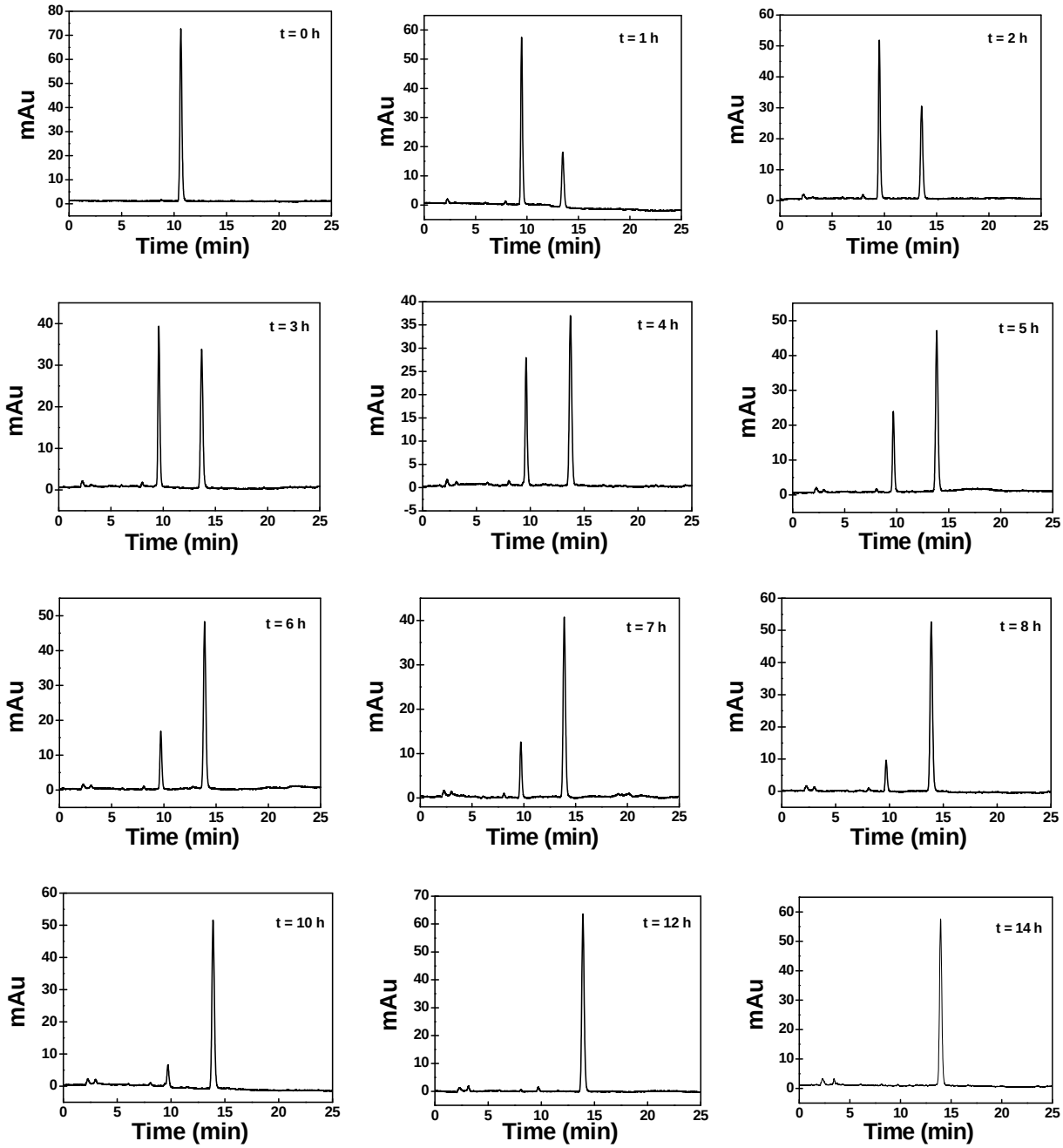

Figure S5. HPLC traces recorded during incubation of **13** in pH 7.4 phosphate buffer shows the formation of **14** as the exclusive product.

Mechanistic Studies

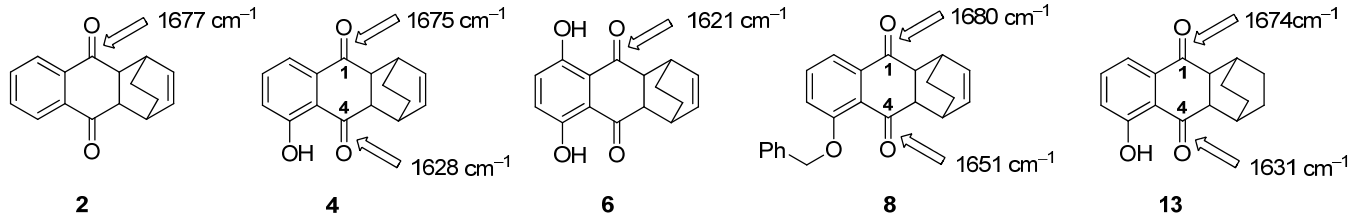

Figure S6. Experimentally determined IR stretching frequencies for carbonyls for **2**, **4**, **6**, **8** and **13**.

Computational calculations. The DFT calculations are being performed with the Gaussian03 program and are analyzed with the help of the GaussView program. The geometries of the model compounds are optimized using the 6-31G basis set, at the DFT level, and these calculations are mainly carried out in the framework of the Becke–Lee–Yang–Parr [B3LYP] functional. Isoelectronic molecular electrostatic potential surfaces (EPS) are plotted by the computer program GaussView. The Mulliken charge density distributions derived from periodic quantum calculation with density functional theory and B3LYP/6-31G(d,p) geometry. Atomic coordinates for compounds **4** and **6** were taken from crystallographic information file (CIF) obtained from the respective X-ray crystal structure data.

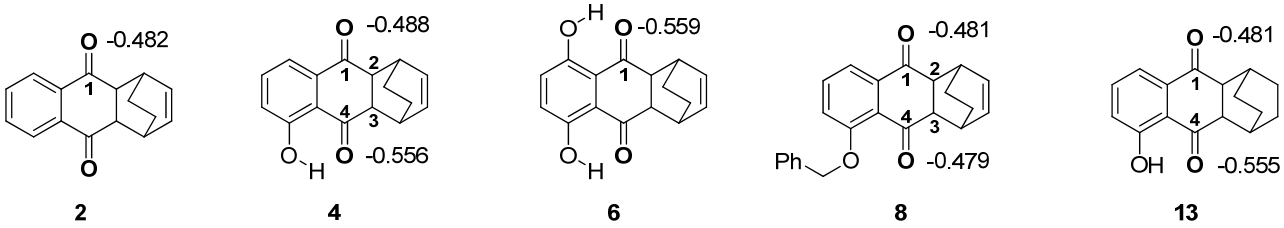

Figure S7. Calculated electronegativities for **2**, **4**, **6**, **8** and **13**.

Crystallographic data: Crystals of compounds **4** and **6** were grown by slow evaporation from a solution of ethylacetae / hexane (25:75 v/v). A single crystal was mounted in a loop with a small amount of the mother liquor. The X-ray data were collected at 296 K temperature on a Bruker AXS SMART APEX CCD diffractometer using MoK α radiation (λ = 0.71073 Å).

Compound **4**, (**C**16H14O3) an orange yellow crystalline needle, ω-scans (θ = 28.91°), for a total number of 3181 independent reflections with a space group *P(-1)* , *a* = 6.536(4), *b* = 10.053(1), *c* = 10.130(1) Å, α = 67.597 (3) , β = 79.986(2), γ = 82.187 (2), *V*= 604.26(15) Å^3, triclinic *P-1*, *Z*=2 for

chemical formula $C_{16}H_{14}O_3$. ρcalcd =1.398 g cm^{-3}, μ = 0.096 mm^{-1}, *F*(000)=268.14, *Rint*=0.0511 for 2161 reflections and *w*R = .1591 (for 3136) reflections. The structure was obtained by direct methods using SHELXS-97. All non-hydrogen atoms were refined anisotropically. The hydrogen atoms were fixed geometrically in the idealized position and refined in the final cycle of refinement as riding over the atoms to which they are bonded. The final *R* value was 0.0511 (*wR* = 0.1591) for 2161, *S* = 0.997. Figure S2a has an ORTEP diagram that was generated using this data.

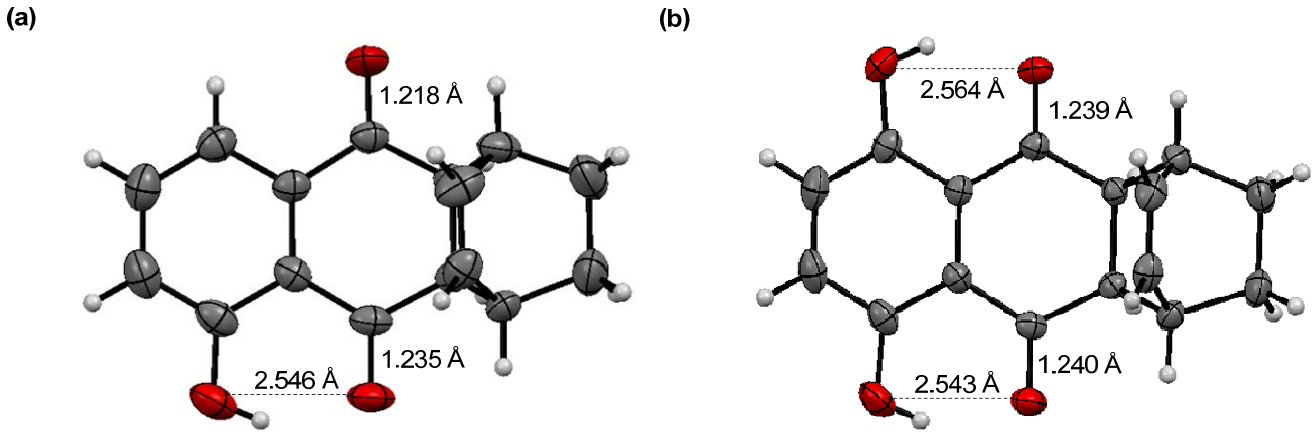

Figure S8. ORTEP diagrams for (a) **4** and (b) **6** shows intramolecular H-bonding between the H-atom of hydroxyl group and the carbonyl oxygen.

Compound **6**, $C_{16}H_{14}O_5$; yellow crystal, ω-scans (θ = 28.68°), for a total number of 3103 independent reflections with a space group *P(-1)* , *a* = 6.410(3), *b* = 9.943(7), *c* = 10.590(5) Å, α = 113.766 (2) , β = 90.148(2), γ = 97.772(2), *V*= 610.93(13) Å^3, triclinic *P-1*, *Z*=2 for chemical formula $C_{16}H_{14}O_5$. ρcalcd =1.469 g cm^{-3}, μ = 0.106 mm^{-1}, *F*(000) = 284.0, *Rint*=0.0388 for 2825 reflections and *w*R = 0.1158 (for 3103) reflections. The structure was obtained by direct methods using SHELXS-97. All non-hydrogen atoms were refined anisotropically. The hydrogen atoms were fixed geometrically in the idealized position and refined in the final cycle of refinement as riding over the atoms to which they are bonded. The final *R* value was 0.0388 (*wR* = 0.1158) for 2825, *S* = 1.045. Figure S2b has an ORTEP diagram that was generated using this data.

Discussion

X-ray diffraction analysis of crystalline **4** and **6** gave O···O bond distances as ~2.54 Å (Fig. S8), which is indicative of intramolecular H-bonding and might similarly result in delocalization of the π-electrons.

Due to these effects, lengthening of the carbonyl bond of C-4 in **4** in comparison with C-1 of **4** might occur (Fig. S8). Indeed, X-ray diffraction analysis shows C-1···O bond distance as 1.218 Å while the C-4···O bond distance was found to be 1.235 Å (Fig. S8a); a similar C···O bond distance (1.24 Å) was recorded for **6** (Fig. S8b). Lengthening of the carbonyl of C-4 in **4** was also confirmed by IR spectroscopy: $\nu_{C=O}$ for **2** was experimentally determined as 1677 cm^{-1} (Fig.S6). C-4 $\nu_{C=O}$ for **4** was significantly diminished to 1628 cm^{-1} and similarly, in the case of **6**, $\nu_{C=O}$ was found as 1621 cm^{-1} (Fig. S6). Thus, intramolecular H-bonding leads to significant reduction of the carbonyl double bond character, which in turn might promote enolate formation leading to increased ROS generation in the cases of **4** and **6**. Removal of H-bonding capability by introduction of a benzyl group resulted in a higher stretching frequency: C-4 $\nu_{C=O}$ for **8** was found as 1651 cm^{-1} (Fig. S6); and this compound generated diminished ROS in comparison with **4** (Figure 1). The aforementioned observations support a proposed mechanism based on enolization of **4** to produce enolates **A1** (path **a**) and/or **A2** (path **b**) as the first step (Scheme S1). The bis-enolate **B1** is produced from **A1** or **A2** which can react with oxygen to generate superoxide by a 1 e^- transfer to produce **B2** (Scheme S1). **B2** can further transfer an additional electron to superoxide to produce hydrogen peroxide and the quinone **4a** (Scheme S1). Enhanced single bond character of the C-4 carbonyl (path **b**) might lower the barrier for enolization in comparison with a similar process for **2** and might help explain increased ROS production during incubation of analogues with proximal hydroxyl groups.

Scheme S1. Proposed mechanism for ROS generation during incubation of 2,3-dihydro-1,4-benzoquinones in aerobic pH 7.4 buffer.

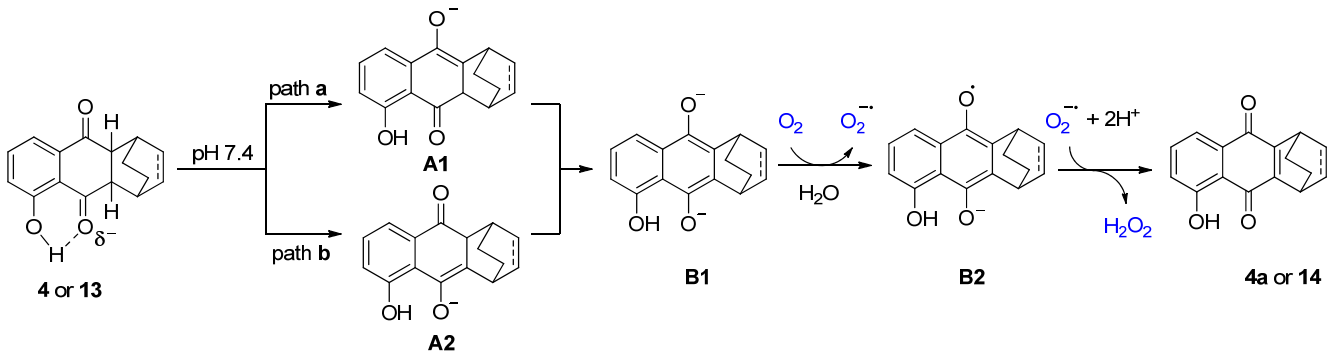

Further support for preferential enolization via path **b** was obtained from computational studies. Energy minimization on **2**, **4**, **6** and **8** using DFT-B3LYP-631G (d,p) was carried out and electron density maps were generated .[43] Here, we found an increased electronegativity (–0.556 versus –0.480) on the oxygen of carbonyls adjacent to a hydroxyl group suggesting an increased partial negative charge on this oxygen (Fig. S7), which might favor enolization (Scheme S1) at C-3, C-4 (path **b**) in comparison with C1-C2 (path **a**). Based on our data, it appears that relative ease of enolization of 2,3-dihydro-1,4-naphthoquinones determined propensity for ROS generation during incubation in aerobic buffer. Enolization of **3** would result in the formation of a double bond attached to a 5-membered ring which might be less favorable (angle strain) than a similar process next to a six-membered ring (in **4**). This effect might help rationalize higher levels of ROS generation from **4** in comparison with **3** (Figure 1).

Cyclic voltammetry. CV analysis was performed using a Basi Epsilon –EC-Ver 2.00.71-USB Bioanalytical systems. A three-electrode setup was used: Pt wire auxiliary electrode, platinum disc working electrode, and $Ag/AgNO_3$ reference electrode. All potential values were calibrated against the saturated calomel electrode (SCE) by measuring the oxidation of ferrocene as a reference ($E°$ (Fc^+/Fc) = 0.424 V vs SCE). The working electrode was polished with 0.05 μM alumina (BASi polishing solution) on a felt pad and washed with de-ionized water and rinsed using acetonitrile. All electrochemical samples were purged with N_2 for 5 min and were measured under a nitrogen atmosphere. The supporting electrolyte of 0.1 M tetrabutylammonium hexafluorophosphate (TBAPF6) and 0.5 mM stock solution of the compound was prepared in MeCN.

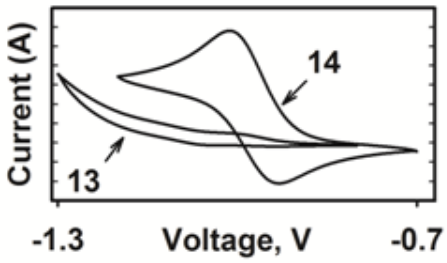

Figure S9. Cyclic voltammogram of **13** and **14**. Conditions: Pt disc working electrode; Pt wire auxiliary electrode; $Ag/AgNO_3$ reference electrode; scan rate =25 mV/s; NBu_4PF_6 = 100 mM as the background electrolyte in MeCN.

This journal is © The Royal Society of Chemistry 2012

Cell Biological and Microbiological Assays

Antimycobacterial Activity Assay. Ten-fold serial dilutions of each test compound/drug were prepared and incorporated into Middlebrook 7H11 agar medium with OADC growth supplement. Inoculum of *Mycobacterium tuberculosis* $H_{37}R_v$ were prepared from fresh Middlebrook 7H11 agar slants with OADC growth supplement adjusted to 1 mg mL^{-1} (wet weight) in Tween 80 (0.05%) saline diluted to 10^{-2} to give a concentration of approximately 107 cfu mL^{-1}. Five µL of bacterial suspension was spotted into 7H11 agar tubes containing 10-fold serial dilutions of drugs per mL. The tubes were incubated at 37 °C, and final readings were recorded after 28 days. The minimum inhibitory concentration (MIC) is defined as the minimum concentration of compound required to completely inhibit the bacterial growth.

***In vitro* cell viability activity.** Human embryonic kidney cells, HEK293 cells were procured from National Center for Cell Sciences, Pune, India. Cells were grown in DMEM, Supplemented with 10% heat inactivated fetal bovine serum (FBS), 100 IU/ml penicillin, 100 mg/ml streptomycin and 2 mM-glutamine. Cultures were maintained in a humidified atmosphere with 5% CO_2 at 37^0C. The cells were subcultured twice each week, seeding at a density of about 2×10^3 cells/ml. The cells were treated with the compound at 25 µM concentration. Control cells were supplemented with complete tissue culture medium containing DMSO (<0.1% final concentration). Cells were grown in 96-well plate by seeding 5×10^3 cells/mL and incubated at 37 °C, 5% CO_2 for 24 h. A standard (3-(4,5-Dimethylthiazol-2-yl)-2,5-diphenyltetrazolium bromide (MTT) assay was used for quantification of cell proliferation in response to treatment. This assay is based on the ability of metabolically active cells to reduce the tetrazolium salt MTT to water-soluble purplecolored formazan compounds. The intensity of the formed dye, proportional to the number of metabolic active cells, was read at 500 nm using the Perkin Elmer Victor™ 3 multiplate reader. Absorbance was recorded after 72 h incubation.

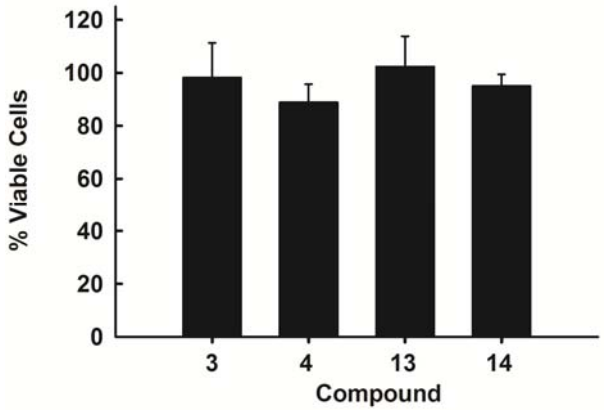

Figure S10. Cell viability assay conducted on selected compounds using human embryonic kidney cells, HEK293 cells. A standard (3-(4,5-Dimethylthiazol-2-yl)-2,5-diphenyltetrazolium bromide (MTT)-based colorimetric assay was conducted. Compounds used are at 25 μM concentration and readings are after 72 h.

Antibacterial Activity of Gram positive and Gram negative bacteria. Anti-bacterial activity of different Gram positive (*Staphylococcus aureus* – SA5021 and *Bacillus subtilis* – BS2063) and Gram negative (*Escherichia coli* – EC2065, *Salmonella typhimurium* – ST2501, *Klebsiella pneumonia* – KP2957 and *Pseudomonas aeruginosa* – PA5029) bacterial strains were measured by a liquid growth inhibition assay. The bacteria were grown in freshly prepared nutrient broth (NB) at 37 ºC for 14–16h. *Mycobacterium smegmatis* - MC^2155, was cultured in middlebrook 7H9 media at 37 °C for 60 h. 100 μL of a logarithmic phase culture of the tested bacteria which was diluted to $10^5 \pm 10^6$ colony-forming units (cfu) per mL were aliquoted in to a 96-well microtiter plate in triplicate, a final concentration of 100 μg mL^{-1} of compound **13** in NB (0.5% DMSO) was added to the above bacterial solution, 0.5% DMSO was used as control. After 24 h of incubation at 37 ºC optical density was measured at 550 nm using Thermo Varioscan microplate reader.

Table S8. Bacterial growth inhibitory activity of **13** at 100 μg mL^{-1}

Bacteria	% Bacterial growth[a]
Staphylococcus aureus	88[b]
Bacillus subtilis	62[b]
Escherichia coli	95[b]
Salmonella typhimurium	99[b]
Klebsiella pneumonia	57[b]
Pseudomonas aeruginosa	87[b]
Mycobacterium smegmatis	74[c]

[a]% of bacterial growth was measured after 24 h of incubation with 100 μg mL^{-1} of compound **13**; [b]Postive control used was ampicillin whose MIC was 33 μg mL^{-1}); [c]Positive control used was ampicillin whose MIC was 11 μg mL^{-1}).

References:

(1) Keshavaraja, A.; Ramaswamy, A. V.; Pandey, B.; Hegde, V. R.; Kumar, P.; Ravindranathan, T. *Angew. Chem.* **1995**, *107*, 2333.
(2) Carreno, M. C.; Garcia Ruano, J. L.; Urbano, A. *J. Org. Chem.* **1992**, *57*, 6870.
(3) Valderrama, J. A.; Espinoza, O.; Gonzalez, M. F.; Tapia, R. A.; Rodriguez, J. A.; Theoduloz, C.; Schmeda-Hirschmann, G. *Tetrahedron* **2006**, *62*, 2631.
(4) Blokzijl, W.; Blandamer, M. J.; Engberts, J. B. F. N. *J. Am. Chem. Soc.* **1991**, *113*, 4241.
(5) Stork, G.; La Clair, J. J.; Spargo, P.; Nargund, R. P.; Totah, N. *J. Am. Chem. Soc.* **1996**, *118*, 5304.
(6) Farina, F.; Paredes, M. C.; Stefani, V. *Tetrahedron* **1986**, *42*, 4309.
(7) Hayakawa, K.; Aso, M.; Kanematsu, K. *J. Org. Chem.* **1985**, *50*, 2036.
(8) Pandey, B.; Dalvi, P. V. *Angew. Chem. Int. Ed.* **1993**, *32*, 1612.
(9) Rathore, R.; Kochi, J. K. *J. Org. Chem.* **1995**, *60*, 4399.
(10) Valiulin, R. A.; Arisco, T. M.; Kutateladze, A. G. *Org. Lett.* **2010**, *12*, 3398.
(11) Eastgate, M. D.; Buono, F. G. *Angew. Chem. Int. Ed.* **2009**, *48*, 5958.
(12) Mori, K.; Hara, T.; Mizugaki, T.; Ebitani, K.; Kaneda, K. *J. Am. Chem. Soc.* **2003**, *125*, 11460.
(13) Ogasawara, Y.; Uchida, S.; Yamaguchi, K.; Mizuno, N. *Chem. Euro. J.* **2009**, *15*, 4343.
(14) Bensinger, R. E.; Johnson, C. M. *Anal. Biochem.* **1981**, *116*, 142.
(15) Trung Pham, H.; Marquetty, C.; Pasquier, C.; Hakim, J. *Anal. Biochem.* **1984**, *142*, 467.
(16) Cho, Y. S.; Kim, H. S.; Kim, C. H.; Cheon, H. G. *Anal. Biochem.* **2006**, *351*, 62.
(17) Dharmaraja, A. T.; Dash, T. K.; Konkimalla, V. B.; Chakrapani, H. *Med. Chem. Comm* **2012**, *3*, 219
(18) Zhou, M.; Diwu, Z.; Panchuk-Voloshina, N.; Haugland, R. P. *Anal. Biochem.* **1997**, *253*, 162.

HPLC Traces in support of purity

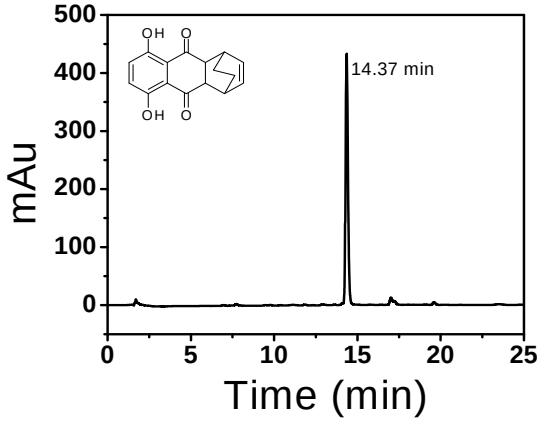

Figure S11. HPLC trace of Compound **6**

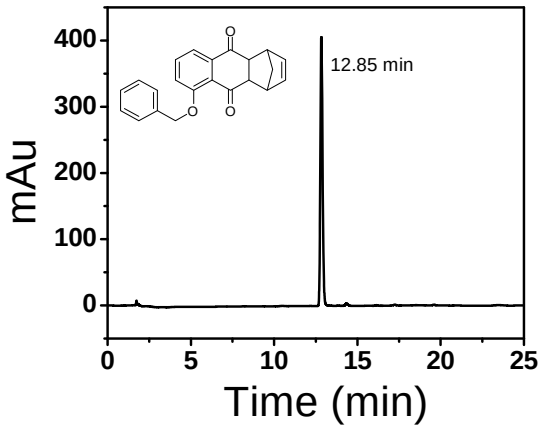

Figure S12. HPLC trace of Compound **7**

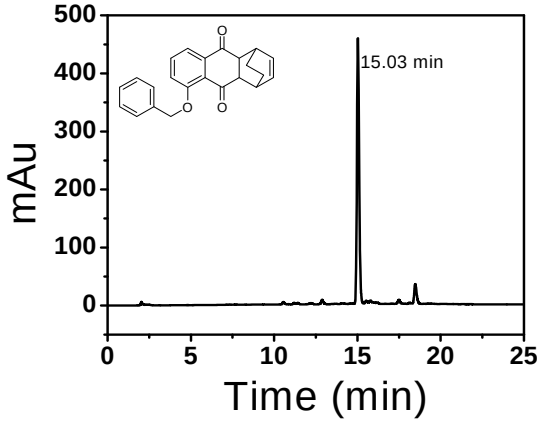

Figure S13. HPLC trace of Compound **8**

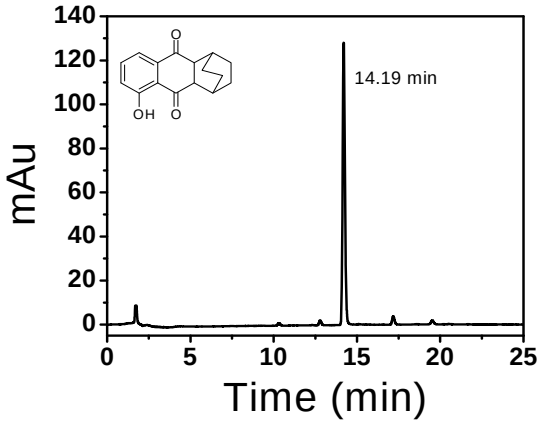

Figure S14. HPLC trace of Compound **13**

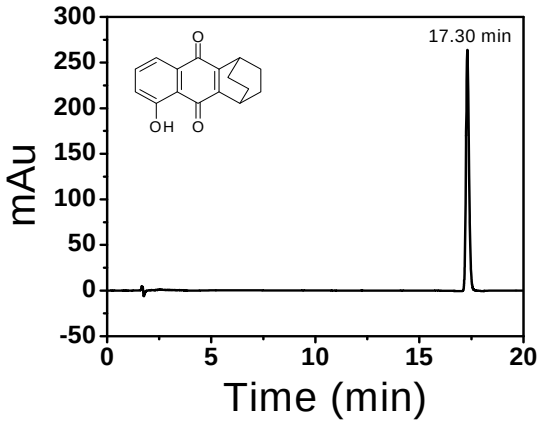

Figure S15. HPLC trace of Compound **14**

NMR Spectra:

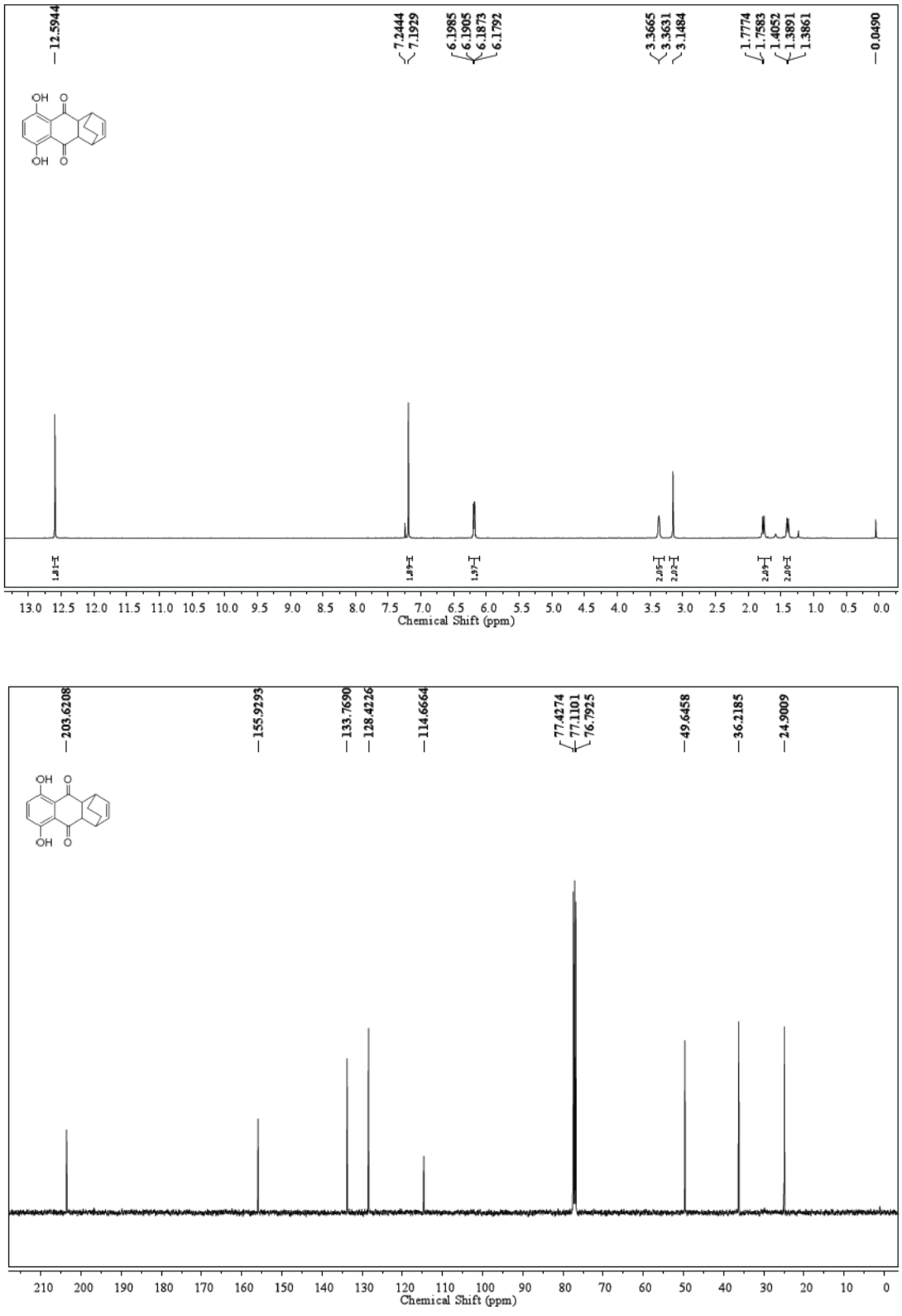

Figure S16. ^{1}H and ^{13}C NMR spectra of compound **6**

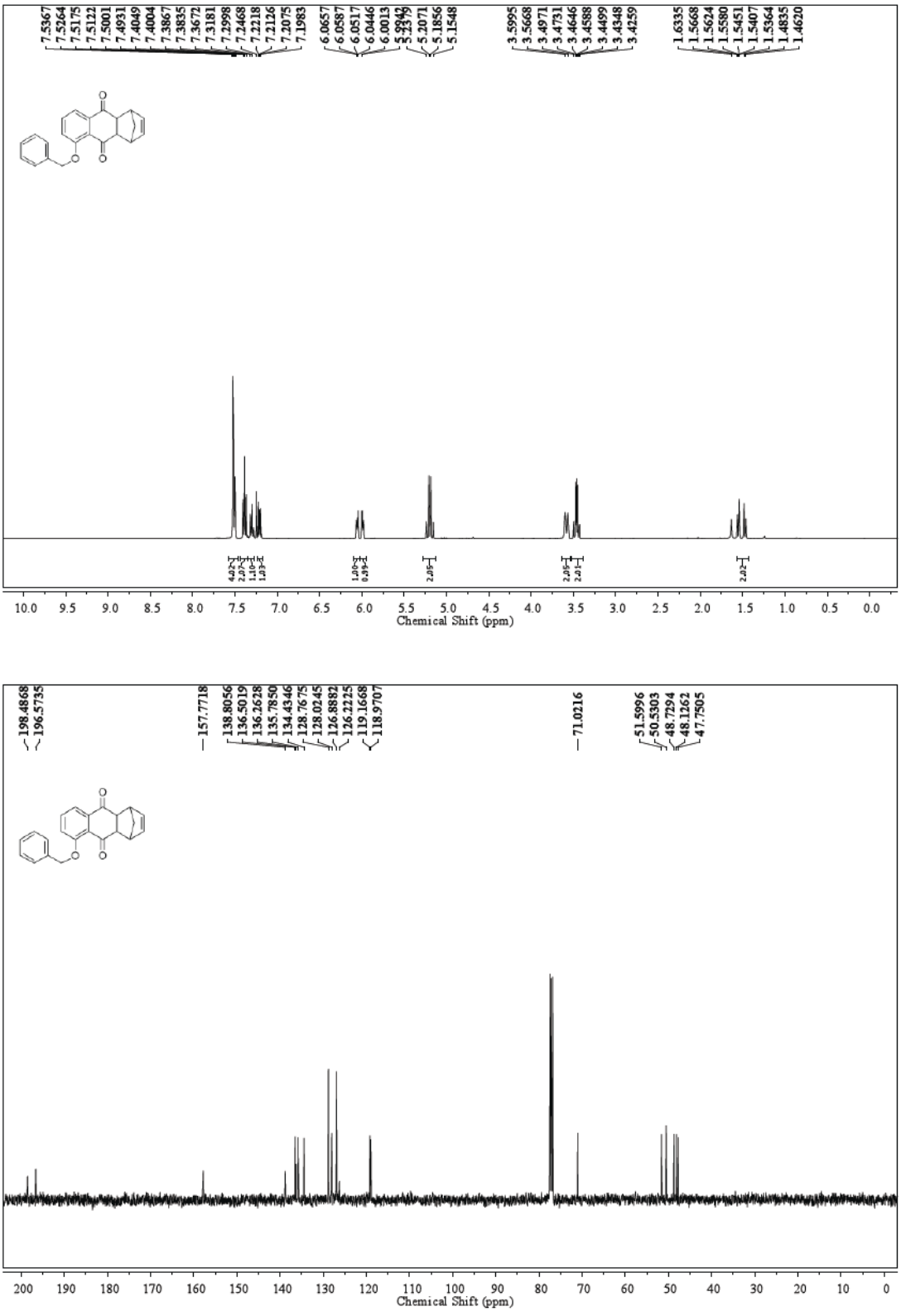

Figure S17. ^{1}H and ^{13}C NMR spectra of compound **7**

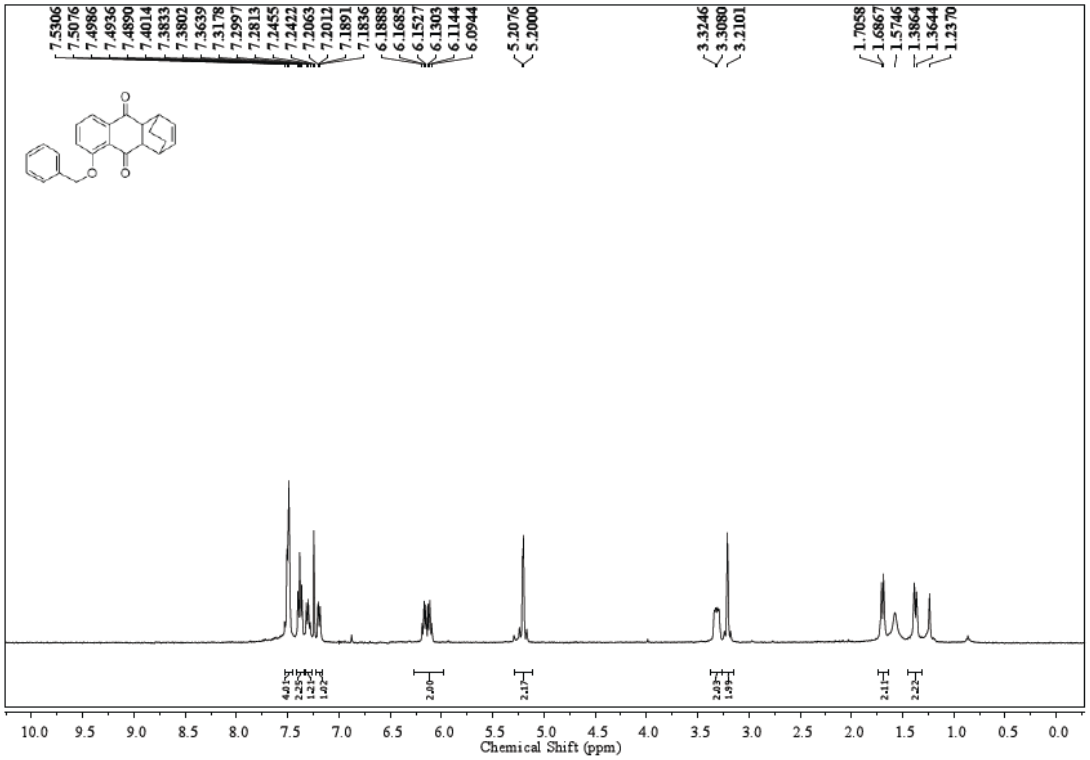

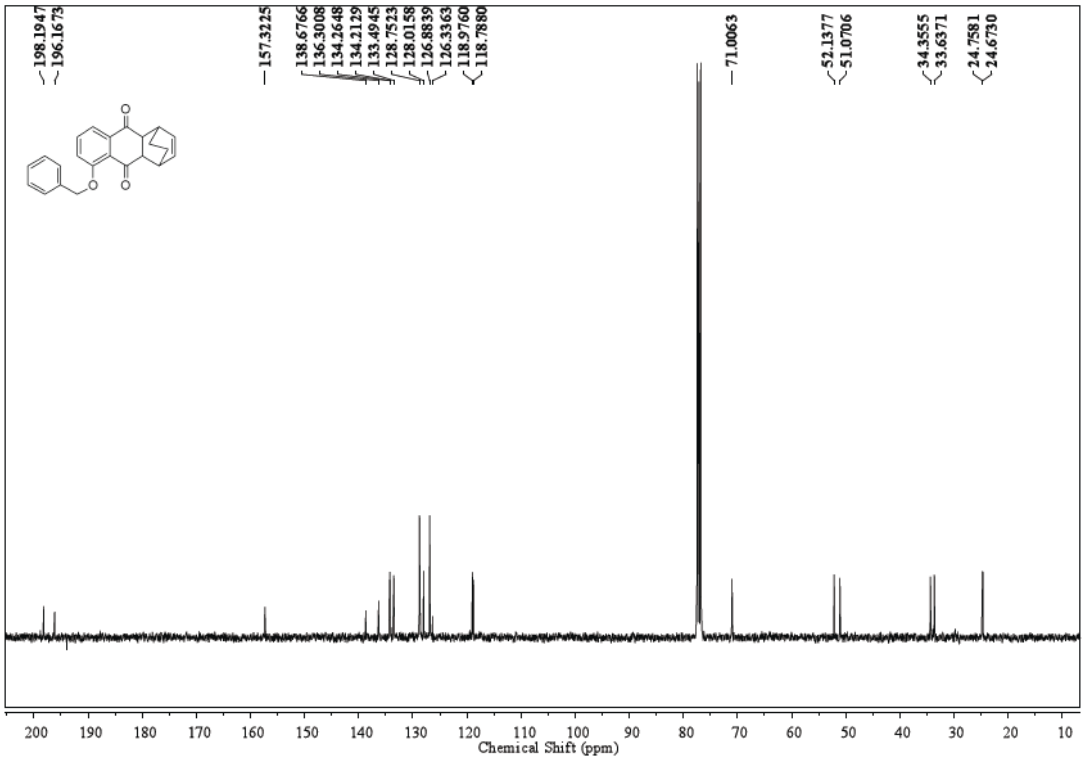

Figure S18. ^{1}H and ^{13}C NMR spectra of compound **8**

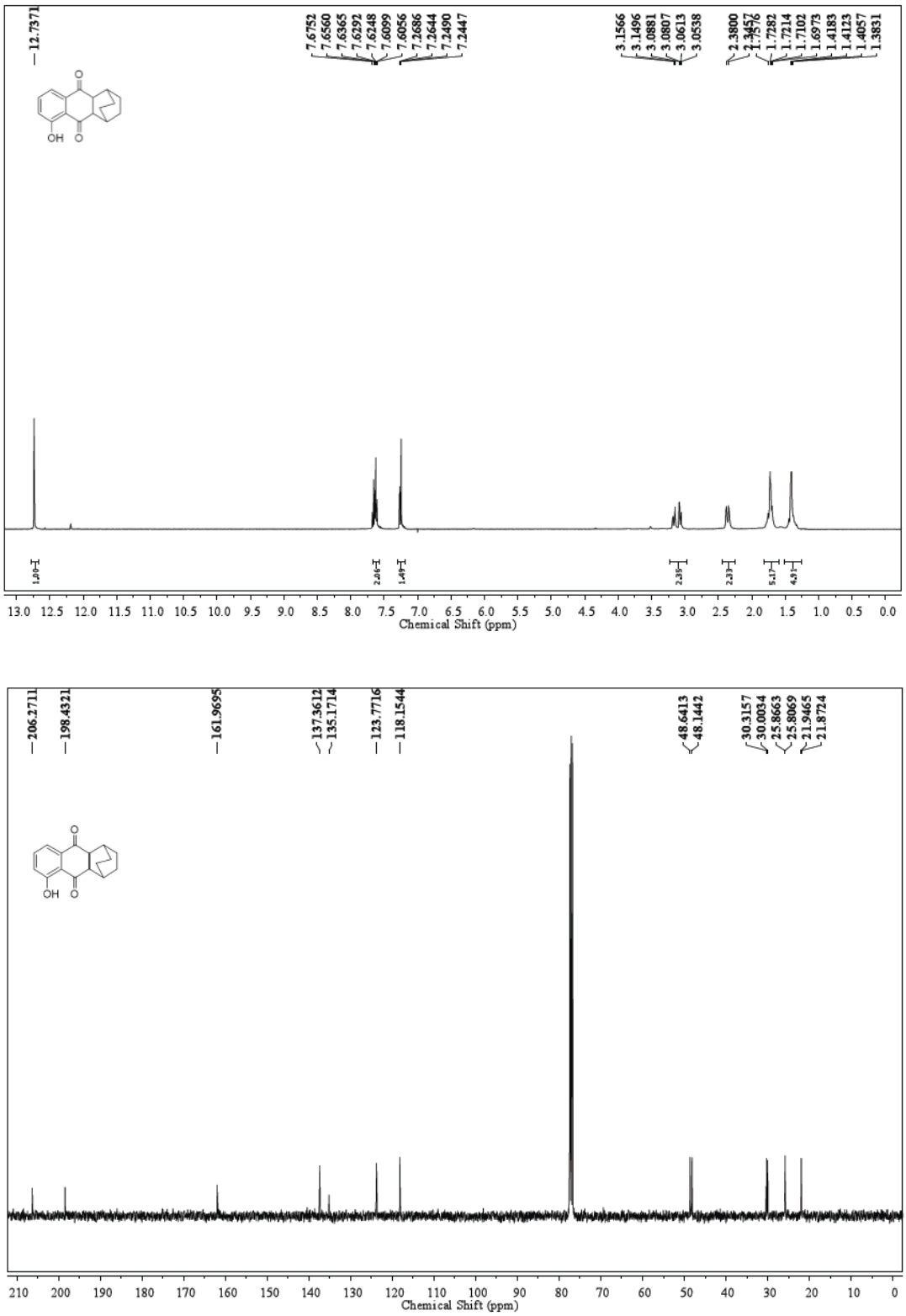

Figure S19. ^{1}H and ^{13}C NMR spectra of compound **13**

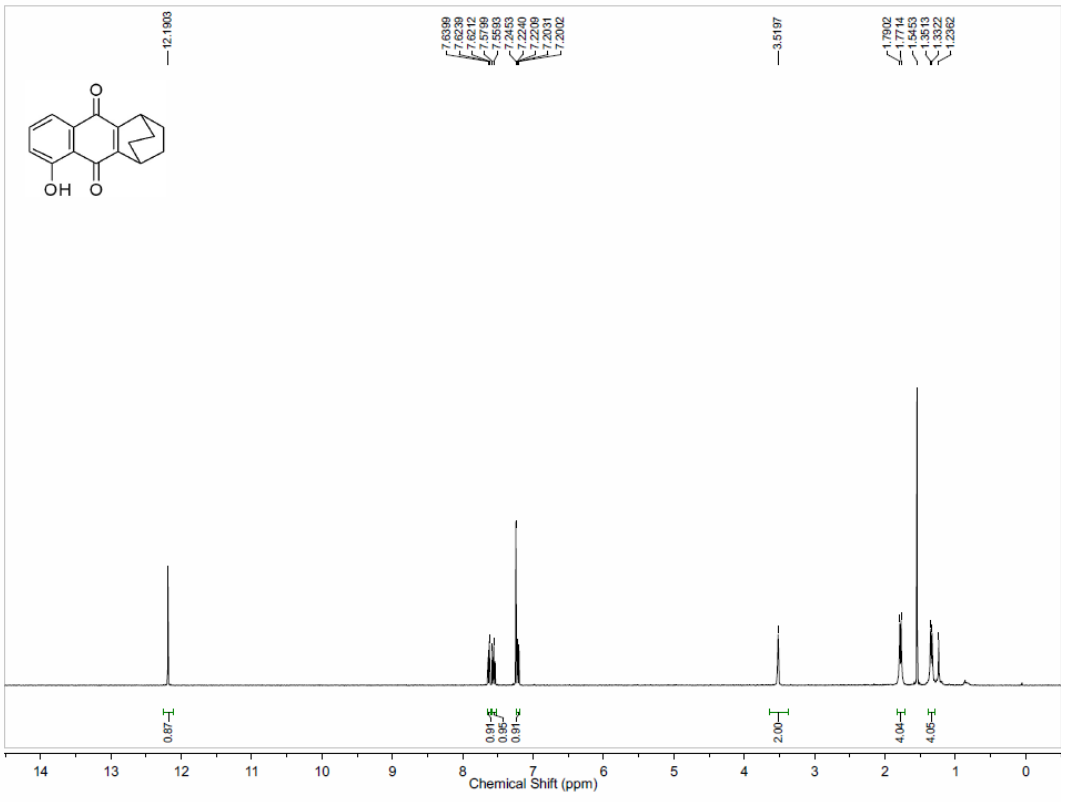

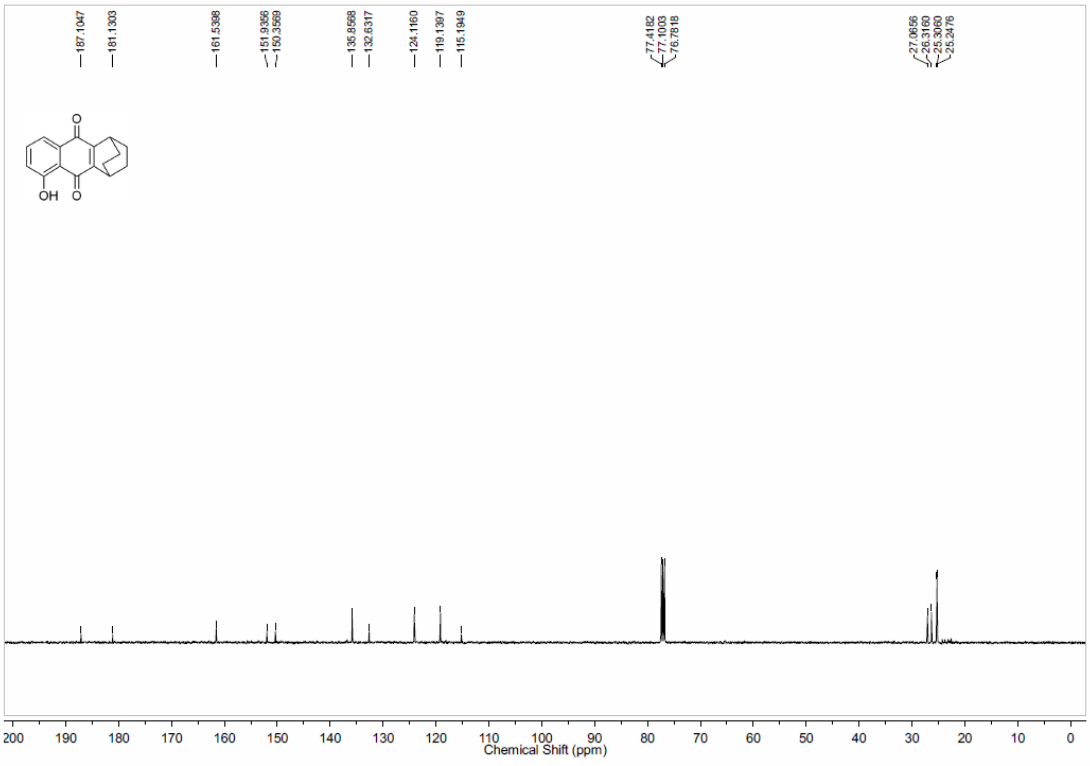

Figure S20. ^{1}H and ^{13}C NMR spectra of compound **14.**